SUPPLEMENTARY INFORMATION

Polypropylene microplastics degradation using ultraporous polarized hydroxyapatite and sun

Jordi Sans,*[a] Marc Arnau,[b,c] and Carlos Alemán*[a,b,c]

[a] Institute for Bioengineering of Catalonia (IBEC), The Barcelona Institute of Science and Technology, Baldiri Reixac 10-12, 08028 Barcelona, Spain

[b] Barcelona Research Center in Multiscale Science and Engineering, Universitat Politècnica de Catalunya - BarcelonaTech, 08930 Barcelona, Spain.

[c] IMEM-BRT Group, Departament d'Enginyeria Química, EEBE, Universitat Politècnica de Catalunya - BarcelonaTech, C/ Eduard Maristany, 10-14, 08019, Barcelona, Spain.

E-mail: jsans@ibecbarcelona.eu and carlos.aleman@upc.edu

METHODS

Materials

Calcium nitrate $Ca(NO_3)_2$, diammomium hydrogen phosphate [$(NH_4)_2HPO_4$; purity > 99.0%], ammonium hydroxide solution 30% [NH_4OH; purity: 28-30% w/w], and polypropylene microplastics (PP MPs; M_n = 50000 and M_W = 190000) were purchased from Sigma Aldrich. Ethanol (purity > 99.5%) was purchased from Scharlab.

Synthesis of Hydroxyapatite (HAp)

A 0.5 M $(NH_4)_2HPO_4$ de-ionized water solution (15 mL) was slowly added (2 mL/min) to a 0.5 M of $Ca(NO_3)_2$ ethanol solution (25 mL) with pH 11 (basified with NH_4OH). The mixture was left aging for 1 h under gentle agitation (150 rpm) at room temperature. Hydrothermal treatment at 150 ºC was applied using an autoclave Digestec DAB–2 for 24 h. The autoclave was allowed to cool down before opening. The precipitates were separated by centrifugation and washed with water and a 60/40 v/v mixture of ethanol/water (twice). A white powder was obtained after freeze-drying for 3 days. The HAp powder was extensively grinded to reduce aggregates and homogenize the grain size, this step being crucial to produce nanoporous HAp samples (see below).

Preparation of ultraporous calcined HAp (c-HAp)

25 g of Pluronic® F-127 polymer were mixed with 25 g of distilled water using a FlackTek SpeedMixer at 3500 rpm for 5 minutes. Then, 50 g of Pluronic® polymer were added and vigorously stirred using the same conditions. The resultant hydrogel was stored at 4 ºC. HAp powder synthesized as described previously was extensively grinded to reduce aggregates and homogenize the grain size. Then, 60% wt. of previously prepared Pluronic® F-127 hydrogel was slowly added to the grinded HAp power in a cold room at

4 ºC. In order to achieve a homogeneous mixture, such addition process was periodically interrupted for stirring at 2500 rpm for 2 min using a Fisherbrand™ Digital Vortex Mixer. The obtained white paste was left aging at 4 ºC for 24 h to ensure the homogeneous distribution of the hydrogel. The resulting ink was shaped modeled using a cold spatula (< 4 ºC) to obtain disc-shaped HAp samples. The utilization of the cold spatula allowed to reduce the friction between the metal and the paste without compromising the homogeneity of the shaped samples. Finally, the samples were calcined at 1000 ºC using a muffle Carbolite ELF11/6B/301 for 2 h. In this step, the Pluronic® F-127 hydrogel was completely removed from the modeled discs.

Thermal polarization for the catalytic activation of c-HAp

c-HAp discs were transformed into upp-HAp discs by placing the samples between two stainless steel plates (AISI 304), which acted as electrodes. The c-HAp sample was left in contact with the negative electrode, while the positive electrode was separated 4 cm from the c-HAp disc. A constant DC voltage of 500 V was applied for 1 h with a GAMMA power supply, while the temperature was kept at 1000 ºC. Samples were allowed to cool down maintaining the applied electric field for 30 min, and finally, all the system was powered off and left to cool down overnight.

Characterization of the catalyst

Wide angle X-ray scattering (WAXS) studies were conducted using a Brucker D8 Advance model with Bragg-Brentano 2θ configuration and Cu K_α radiation (λ = 0.1542 nm). Measurements were performed in a 2θ range of 20º –60º in steps of 0.02º, and a scan speed of 2 s using a one-dimensional Lynx Eye detector.

Raman analyses were performed by means of an inVia Qontor confocal Raman microscope (Renishaw) equipped with a Renishaw Centrus 2957T2 detector and a 532 nm laser. In order to obtain representative data, 32 single point spectra were averaged.

Electrochemical impedance spectroscopy (EIS) studies were performed using a VIONIC potentiostat (dry samples) and a Multi Autolab/M101 (wet samples) both from Metrohm connected to a conductivity meter cell by means of two stainless steel electrodes AISI 304 isolated by a resin holder.[S4] Measurements, which were performed in the 1 MHz – 10 mHz frequency range and applying a 100 mV sinusoidal voltage, were conducted considering both dry and wet c-HAp and upp-HAp pellets. Wet samples were prepared by dispensing approximately 50 μL of a 3.5 % NaCl on c-HAp and pp-HAp/Bru pellets. Samples were placed between the two electrodes and EIS measurements were performed. Electrical equivalent circuits (EECs) were obtained by fitting the experimental data. The maximum change in the quadratic least square error (χ^2) of the fit was defined as the convergence criterion. The fitting was considered successfully converged when the absolute change in χ^2 was lower than 0.001.

Morphological characterization was performed by scanning electron microscopy (SEM) using a Focused Ion Beam Zeiss Neon40 microscope equipped with a SEM GEMINI column with a Shottky field emission. Samples were sputter-coated with a thin layer of carbon to prevent sample charging problems.

Brunner-Emmett-Teller (BET) surface area analysis were performed with a Micrometrics ASAP 2000 system using N_2 and with sample degasification conditions consisting of 1 h at 90 ºC followed by 4 h at 300 ºC to ensure complete gas desorption from the samples. The surface area was calculated using the BET model and the pore size diameter using the desorption isotherm through Barrett-Joyner-Halenda (BJH) model.

High-resolution transmission electron experiments were carried out in a JEOL JEM J2100 microscope, equipped with a LaB6 thermionic electron gun and operated at an accelerating voltage of 200 keV. Images were recorded using a Gatan Orius CCD camera.

Catalytic conversion of PP into alcohols

To carry out the catalytic conversion of PP, upp-HAp (20 mg) was contacted with PP MPs (30 mg) in a holder (see Figure S4). The addition of milli-Q water content was controlled depending on the reaction conditions as: 1) Immersed: 200 μL of milli-Q water were added, immersing completely PP and upp-HAp; 2) Wet: 200 μL of milli-Q water were firstly added and subsequently removed, leaving only the water adsorbed in the surface and bulk of upp-HAp; and 3) Dry: no liquid milli-Q water is added to the reaction. Finally, samples were exposed to sunlight (SunLite Solar Simulator from ABET technologies, equipped with a 100 W xenon arc lamp) irradiation during 15 minutes to 4 hours. Note that no extra temperature, pressure or electrical currents were applied during the reaction. The power of the solar light irradiation was calibrated using as reference AM 1.5G earth's surface level.

Characterization of the reaction products

The characterization of the reaction products was performed by ^{1}H NMR studies. Accordingly, the PP degradation was assessed from the determination of carbon compounds dissolved in water. Therefore, while for immersed samples 50 μL were collected for their analyses, for wet and dry conditions samples were re-suspended in 200 μL of milli-Q water to dissolve all the generated degradation products. The ^{1}H NMR spectra were acquired with a Bruker NMR Ascend 400 spectrometer operating at 400.1 MHz. Deuterated water and tetramethylsilane, as the internal standard for chemical shift

were added. Unless explicitly said, the yields were calculated by peak area integration acquiring 256 scans in all cases to ensure proper signal-to-noise ratio. *zgcppr* water suppression method was used. Accurate quantification was achieved by regularly calibrating the resulting products (*i.e.* ethanol and isopropanol) through external references.

S1. J. Sans, M. Arnau, V. Sanz, P. Turon, and C. Alemán, *Chem. Eng. J.*, 2022, **433**, 133512.

S2. Z. Iqbal, V. P. Tomaselli, O. Fahrenfeld, K. D. Möller, F. A. Ruszala, E. Kostiner, *J. Phys. Chem. Solids*, 1977, **38**, 923.

S3 J. Sans, V. Sanz, L. J. del Valle, J. Puiggalí, P. Turon, C. Alemán, *J. Catal.*, 2021, **397**, 98.

S4. F. Müller, C. A. Ferreira, D. S. Azambuja, C. Alemán, and E. Armelin, *J. Phys. Chem. B*, 2014, **118**, 1112.

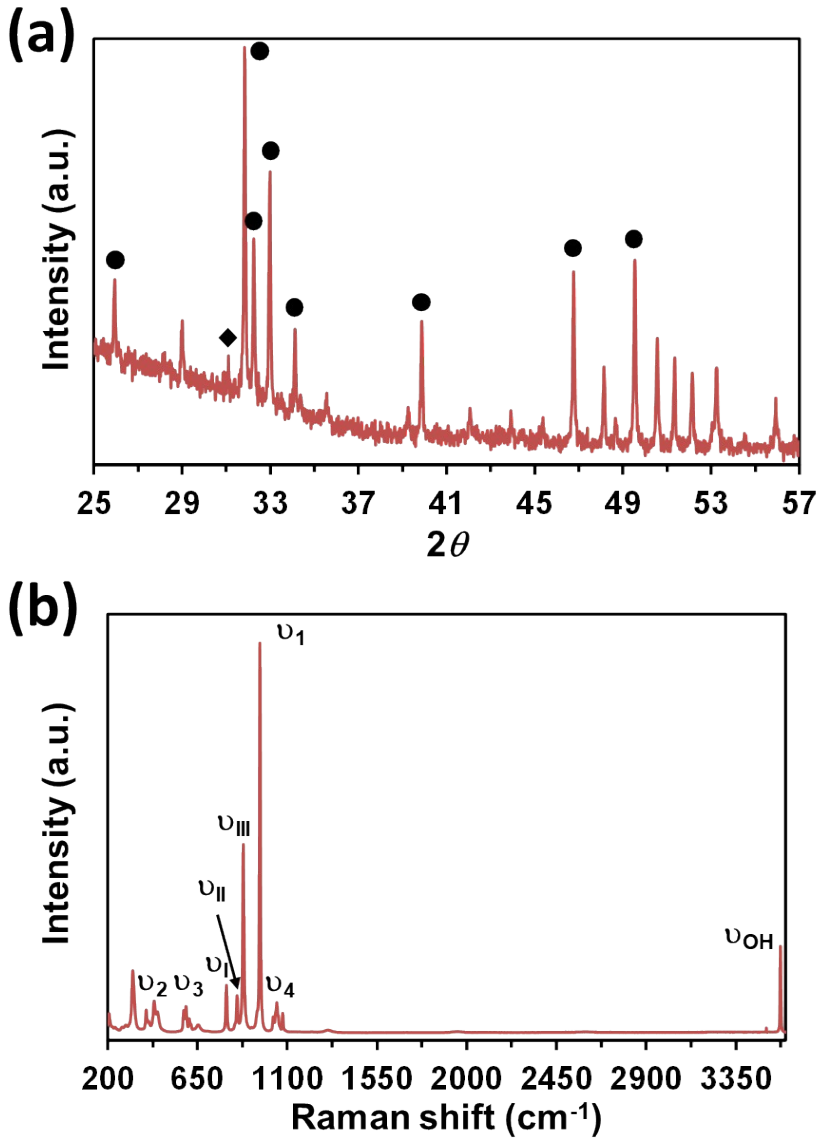

Figure S1. (a) X-ray diffractogram and (b) Raman spectrum for upp-HAp. In (a), the X-ray diffractogram of upp-HAp shows the typical HAp reflections (solid circles) at 2θ = 25.9º (002), 31.8º (211), 32.3º (112) and 33.0º (300), 34.0º (202), 39.8º (310), 46.7º (222), and 49.5º (213), while the presence of brushite (solid diamond) is confirmed by peak at 31.1º (121).[S1] In (b), the Raman spectrum of upp-HAp presents, in addition to the four PO_4^{3-} characteristic peaks and the OH^-stretching vibration of HAp at ν_1 = 962 cm^{-1}, ν_2 = 400-490 cm^{-1}, ν_3 = 570-625 cm^{-1}, ν_4 = 1020-1095 cm^{-1} and ν_{OH}= 3573 cm^{-1},[S2] the three characteristic peaks of brushite at ν_I= 794 cm^{-1} (P–OH rotation mode), ν_{II} = 848 cm^{-1} (P–OH deformation mode) and ν_{III} = 878 cm^{-1} (HPO_4^{2-} vibrations).[S3]

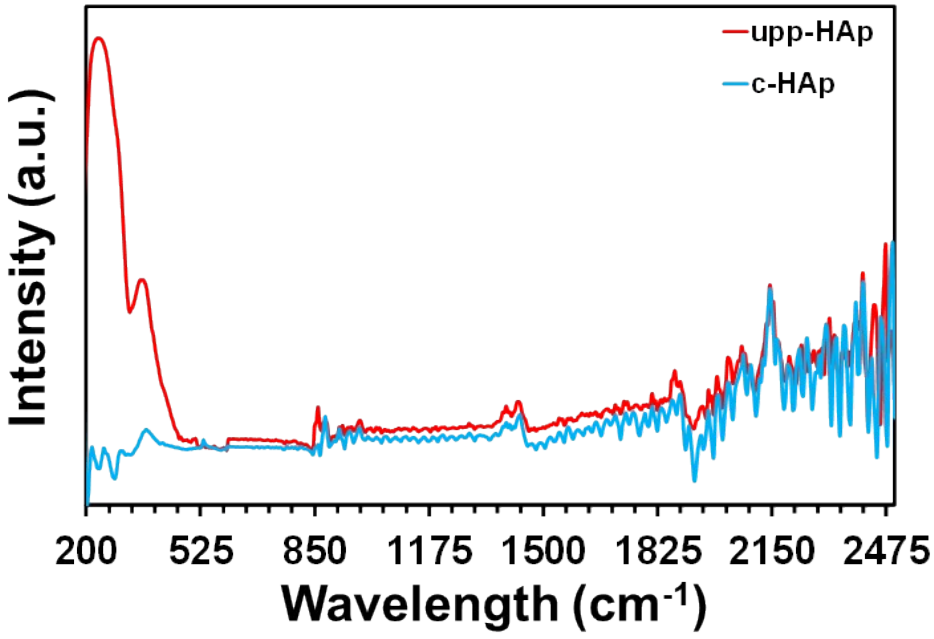

Figure S2. Absorption spectra of upp-HAp and c-HAp.

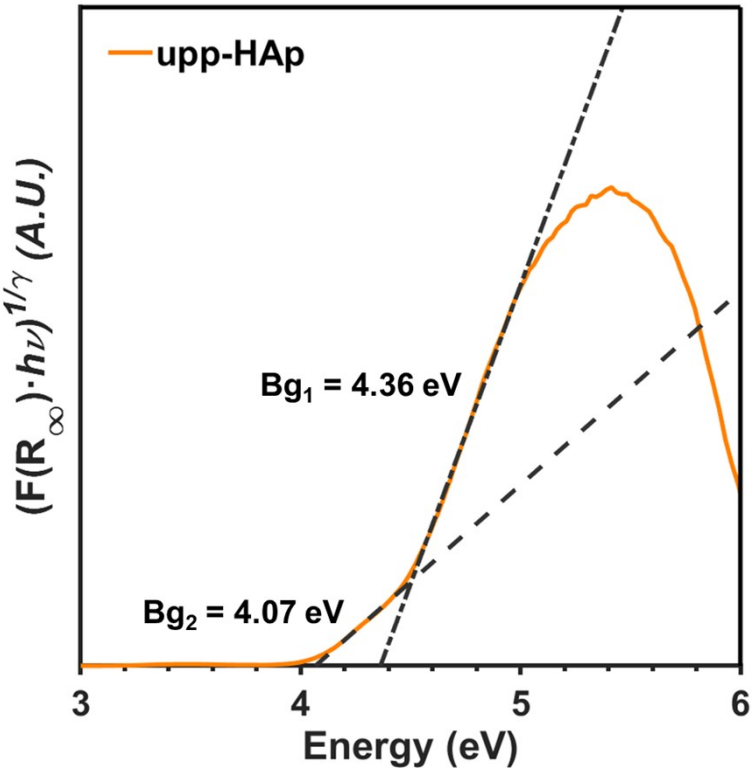

Figure S3. Tauc plot representing Kubelka–Munk function multiplied by the energy ($F(R_\infty)\cdot h\upsilon$) in front of $h\upsilon$. The band gaps (B_g) derived using the procedure proposed by Makuła *et al.*[13] is displayed.

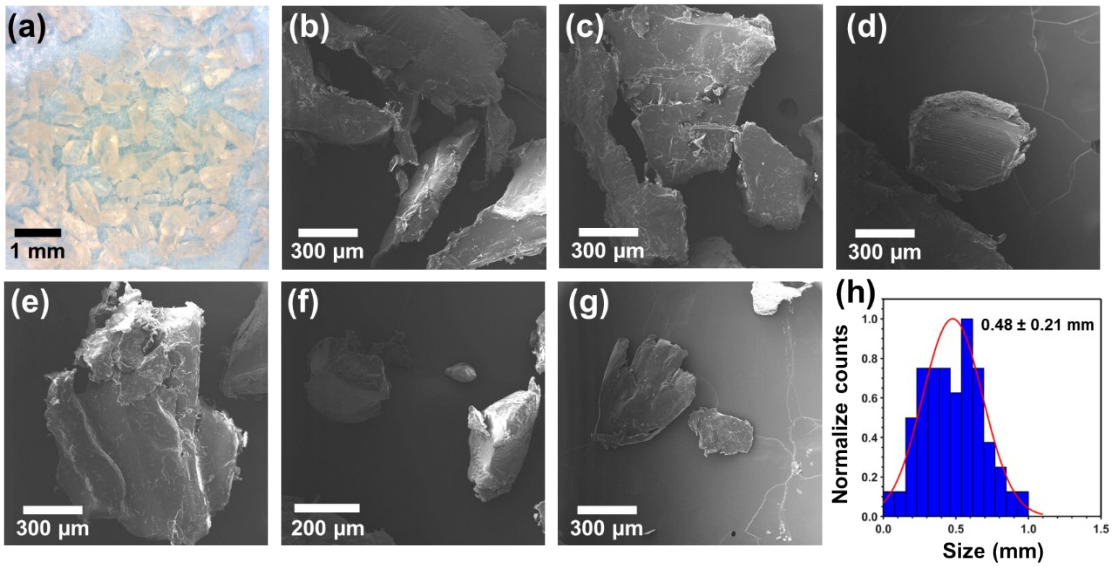

Figure S4. Representative (a) Optical and (b-g) SEM micrographs of grinded PP particles. (h) Size distribution of the PP particles as observed from SEM micrographs.

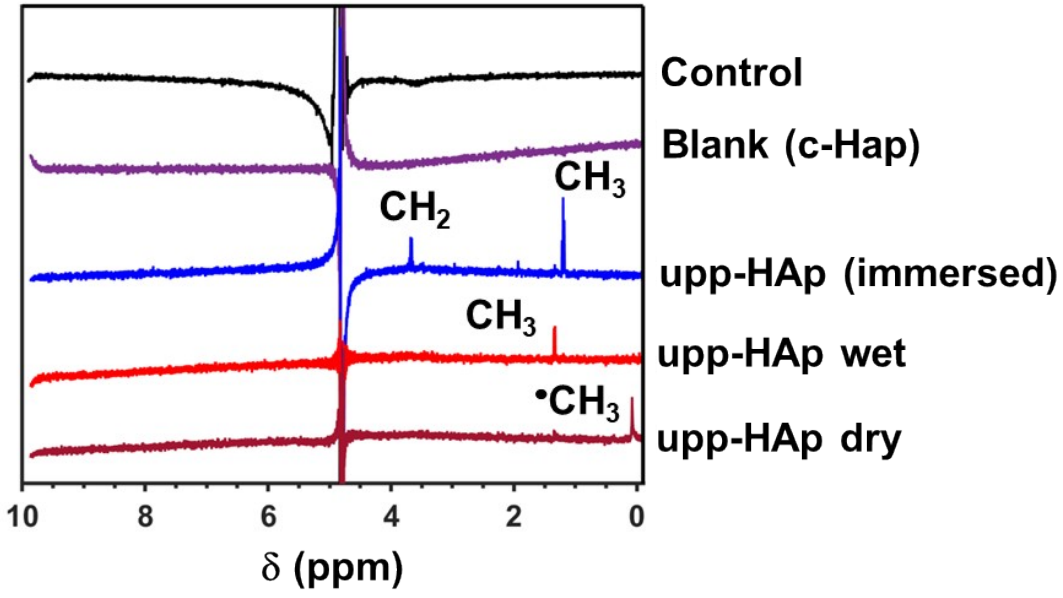

Figure S5. Complete ^{1}H NMR spectra of the control and blank reactions and of reactions with upp-HAp catalyst in immersed, wet and dry conditions. In all cases, reactions were conducted for 2 h at one sun.

Table S1. Data derived from the fitting of the electrochemical impedance spectra recorded for dry c-HAp and upp-HAp. The EECs are displayed in Figure 1a. The statistical error associated with each circuit element is displayed in parenthesis (in %). c-HAp and upp-HAp has been described as a constant phase elements (CPE_b) in parallel with its respective resistance (R_b) and Warburg impedance (W) element. Besides, the HAp phase of upp-HAp was modeled considering a capacitive element (C_b) in parallel with the resistance (R_b), while the brushite phase was described as a constant phase element (CPE_γ) in parallel with its resistance (R_γ) and Warburg impedance (W).

EEC Model	**c-HAp**	**upp-HAp**
R_b (MΩ cm^{-2})	568.66 (2.60%)	9.65 (5.88%)
CPE_b (pF·cm^{-2}·s^{n-1})	20.61 (2.93%)	-
n_b	0.93 (0.29%)	-
R_W (nF·cm^{-2}·$s^{-1/2}$)	2.44 (10.26%)	-
R_γ (MΩ cm^{-2})	-	114.48 (0.88%)
CPE_γ (pF·cm^{-2}·s^{n-1})	-	23.89 (2.65%)
n_γ	-	0.96 (0.26%)
$R_{W\gamma}$ (nF·cm^{-2}·$s^{-1/2}$)	-	7.11 (2.54%)
C_b (pF·cm^{-2})	-	20.7 (3.14%)

Table S2. Data derived from the fitting of the electrochemical impedance spectra recorded for wet c-HAp and upp-HAp. The EECs are displayed in Figure 1b. The statistical error associated with each circuit element is displayed in parenthesis (in %). The elements used to describe c-HAp and upp-HAp are described in Table S1.

EEC Model	**c-HAp**	**upp-HAp**
R_s (MΩ cm^{-2})	40.00 (2.20%)	38.00 (2.50%)
R_γ (kΩ cm^{-2})	-	9.07 (4.84%)
CPE_γ (μF·cm^{-2}·s^{n-1})	-	100.81 (1.75%)
n_γ	-	0.71 (0.27%)
R_b (MΩ cm^{-2})	9.69 (4.81%)	1.57 (5.00%)
C_b (pF·cm^{-2})	2.22 (0.49%)	12.16 (0.66%)
	n =0.83 (CPE) (0.09%)	

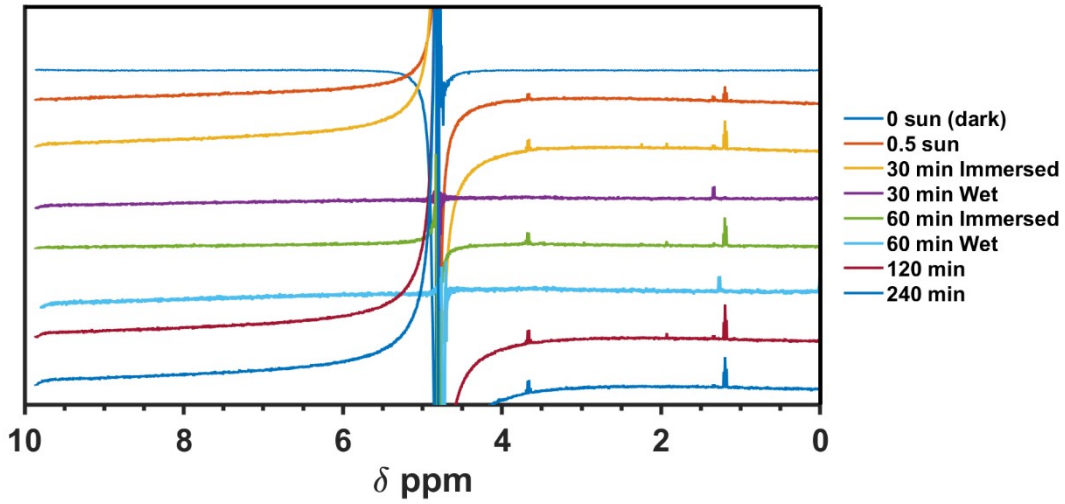

Figure S6. Complete ^{1}H NMR spectra of the reactions used to follow the kinetics of PP MPs conversion into EtOH and ^{i}PrOH using upp-HAp.

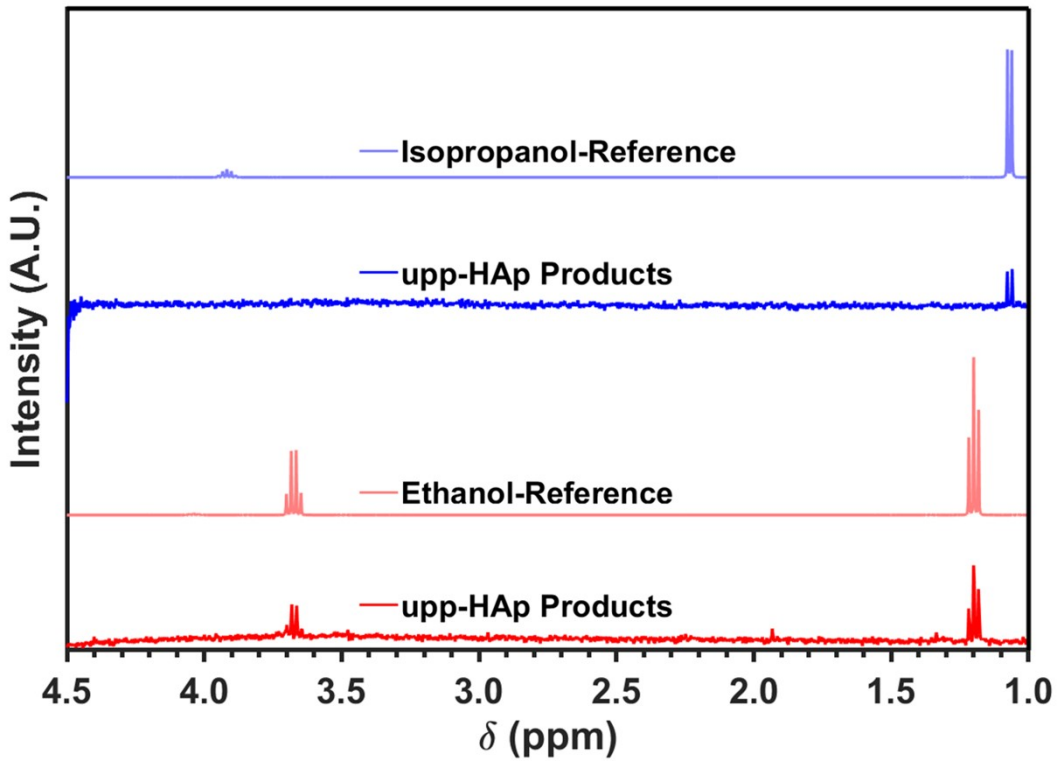

Figure S7. Calibration ^{1}H NMR spectra with external references used for the quantification of the obtained compounds.

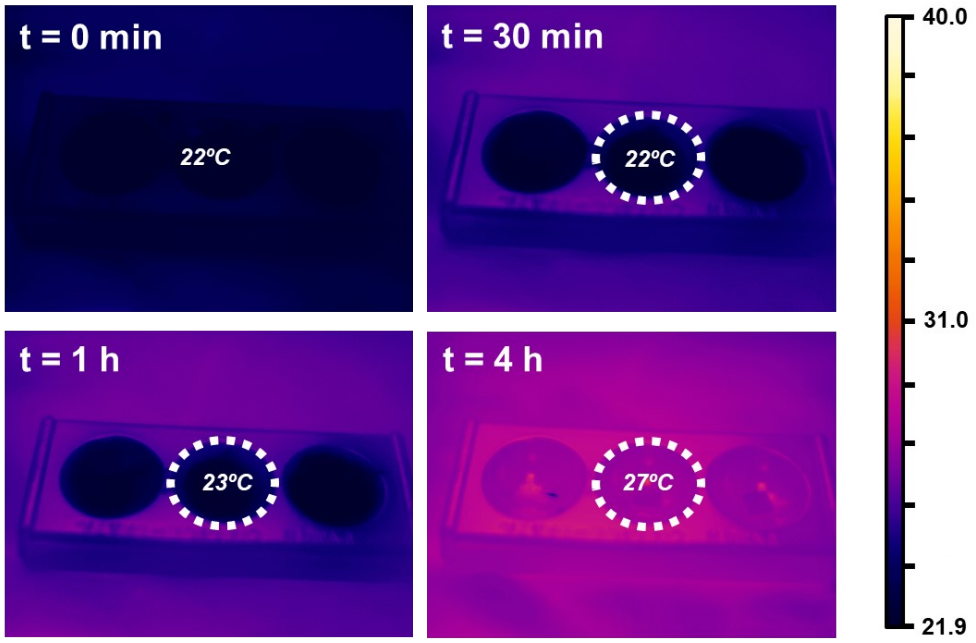

Figure S8. Infrared camera images recorded for the immersed catalytic system, which is constituted by upp-HAp, water and PP waste, under 1 sun irradiation at different times.

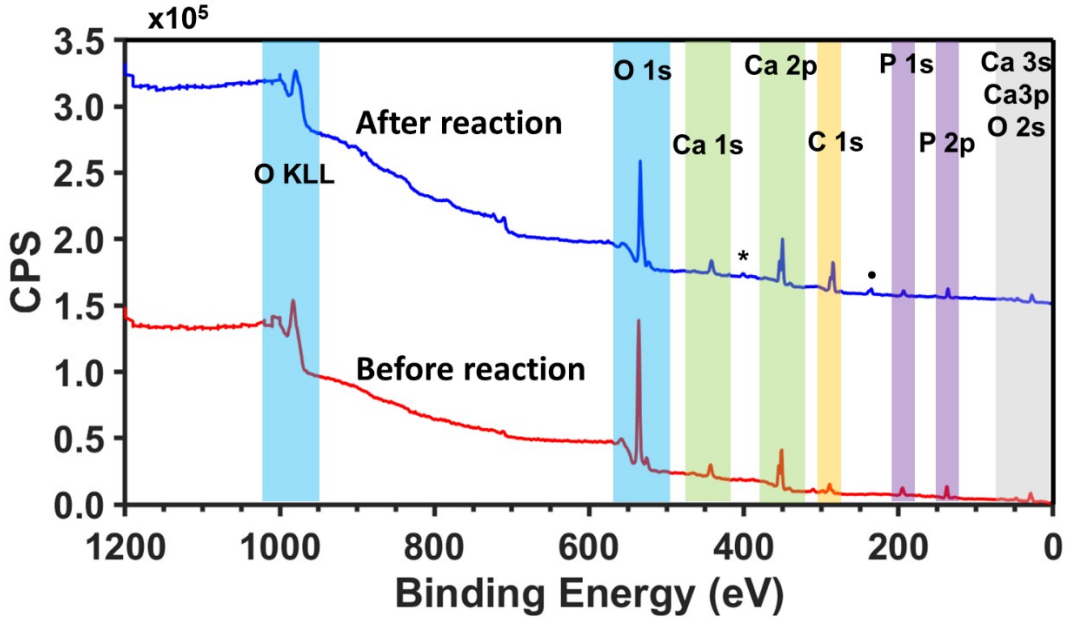

Figure S9. Survey XPS spectrum of upp-HAp after the 2 h reaction in immersed conditions. Absorbed nitrogen peaks are indicated with asterisks.

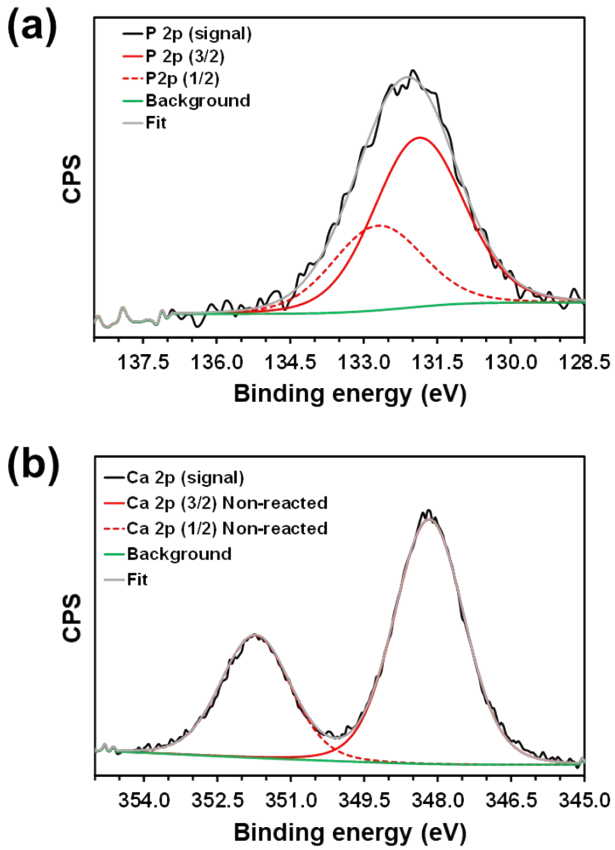

Figure S10. High resolution XPS spectra of upp-HAp before any reaction: (a) P 2p and (b) Ca 2p.

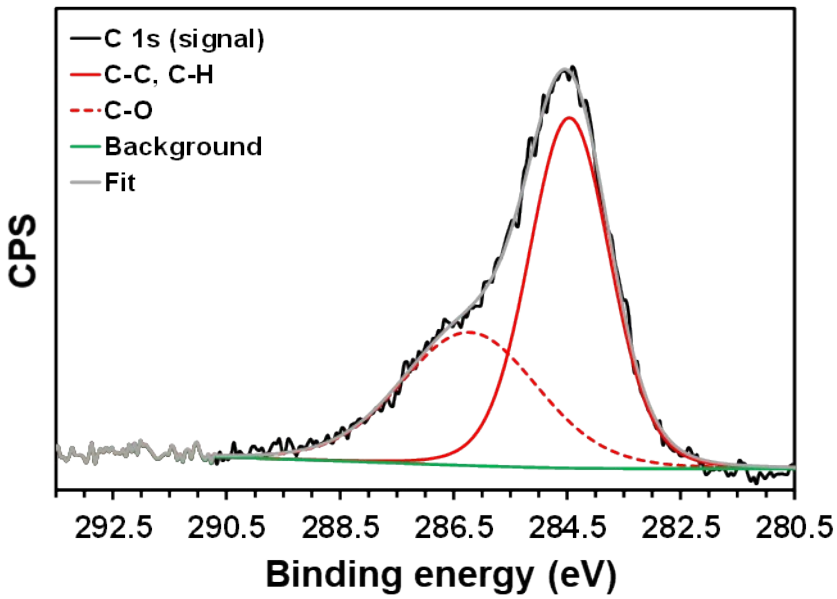

Figure S11. High resolution C 1s XPS spectrum of PP before the reaction.